Asian Journal of Chemistry; Vol. 33, No. 4 (2021), 793-801

ASIAN JOURNAL OF CHEMISTRY

https://doi.org/10.14233/ajchem.2021.23094

Structurally Designed Imine Skeletal Pyrenyl Pendant Pyridine Core Polybenzoxazine nSiO$_2$/PBZ Hybrid Polymer Nanocomposites

S.G. GUNASEKARAN*, L. DEVARAJ STEPHEN, V. ARIVALAGAN and M. SOUNDARRAJAN

Department of Chemistry, SRM Valliammai Engineering College (Autonomous), Kattankulathur-603203, India

*Corresponding author: Fax: +91 44 27451504; Tel.: +91 44 27454784; E-mail: gunasekaransg.chemistry@valliammai.co.in

Received: 9 December 2020; *Accepted*: 30 January 2021; *Published online*: 20 March 2021; AJC-20285

Novel polybenzoxazine-silica (nSiO$_2$/PBZ) hybrid nanocomposites were designed and synthesized using carbazole terminal pyrenyl pyridine core imine skeletal benzoxazine monomer (PYCBZ) and nanosilica (nSiO$_2$) through *in situ* sol-gel method. The FT-IR and Raman spectral studies ascertained the formation of nanosilica reinforced polybenzoxazine hybrid nanocomposites. The nSiO$_2$/PBZ hybrid nanocomposites exhibited excellent thermal stability and higher char yield than that of neat PBZ. The elevation in glass transition temperature of the nanocomposites was evidenced by the limited motion of the polymeric network with the introduction of nanosilica particles in the PBZ matrices. The hydrophobic nature of a less polar nSiO$_2$ in the composites zipped the water uptake behaviour of (nSiO$_2$/PBZ) hybrid nanocomposites to low percentage. The shift in the absorption peak reveals that the nanosilica particles were successfully incorporated through thermal ring opening polymerization of benzoxazine. The homogeneous reinforcement of nSiO$_2$ particles retains the fluorescent properties of polybenzoxazine. The uniform molecular level dispersion of nano SiO$_2$ onto polybenzoxazine networks were confirmed from transmission electron microscope and scanning electron microscope images.

Keywords: Carbazole, Benzoxazine, Nanosilica, Polybenzoxazine, Thermal stability, Photoluminescence, Morphology.

INTRODUCTION

Organic-inorganic nanocomposites are generally organic polymer composites with inorganic nanoscale building blocks. They combine the inorganic material (*e.g.* rigidity, thermal, mechanical stability) and the organic polymer (*e.g.* flexibility, dielectric, water absorptivity, ductility). Moreover, they usually have special properties of nanofillers imperative to materials with amended properties [1]. Organic-inorganic nanocomposites have been considered as a new generation of high performance composite materials. In recent years, various techniques for synthesizing hybrid nanocomposites are prepared [2]. The easy synthetic process of benzoxazine monomers can be considered to provide variety of monomers as well as polymeric composites. The structure and synthesis of nanomaterials with improved properties is a challenging problem. A concerted research on the development of inorganic materials with organic hybrid polymers at a nanoscale level is sketched attention for the past few years [3,4].

Polybenzoxazines, a new class of thermosetting polymers have derived and received much attention due to their good performance and high flexibility in molecular outline [5]. Different kind of raw materials used for the synthesis of benzoxazine monomer give considerable molecular-outline flexibility. Generally, benzoxazine was synthesized by using aliphatic or aromatic phenols or bisphenols, primary amine (aliphatic or aromatic) and formaldehyde solution through Mannich condensation [6]. The polycomposites were obtained by the ring-opening polymerization of ring benzoxazine by thermal curing, without using a catalyst and producing no byproducts. Polybenzoxazine shows better combinations of attractive properties such as flame retardance, heat resistance, cost effectiveness and electrical and electronic properties over the regular composites in many features. They also produce additional unique properties such as high dimensional stability, low water absorption and near-zero volumetric shrinkage or expansion upon curing [7-9].

In past few years, ample amount of studies on the hybridization of polybenzoxazine with various inorganic nanoparticles

to produce polybenzoxazine nanocomposites are reported [10-13]. Other excellent properties of polybenzoxazine nanocomposites include barrier resistance and resistant to catching fire, improvement in optical and electrical properties. Agag & Takeichi [14] reported the first polybenzoxazine nanocomposites by using organic clay as nanoparticles and polybenzoxazine matrix to give polybenzoxazine incorporated clay nanocomposites with better thermomechanical properties. By using polyhedral oligomeric silsesquioxane, Polybenzoxazine-POSS hybrids as different nanocomposites have been also developed [15].

Polybenzoxazine hybrid nanocomposites were prepared by sol-gel process, affording hybrid materials of good thermal stability. The well-known sol-gel process makes it attractive for the application in the synthesis of organic-inorganic hybrid nanocomposites [16-19]. The characteristics of the organic-inorganic hybrids are highly depend on the interaction between the organic polymers and the siloxane matrix [20-25] and their complete distribution within the hybrid systems. Agag *et al.* [25] developed a polybenzoxazine-TiO_2 based hybrid, with enhanced thermal properties [25]. Recently, Gunasekaran *et al.* [26] reported a new polybenzoxazine-silica hybrid nanocomposite using a new benzoxazine monomer with improved thermal stability and increased char yield [26].

In this work, a newly designed triaryl pyridine core imine skeletal benzoxazine monomer was first synthesized from pyrenyl pendant Schiff base/imine. Then, the sol-gel process was employed to incorporate nanosilica nanoparticles with benzoxazine monomers to prepare polybenzoxazine-nanosilica hybrid nanocomposites. The formed polybenzoxazine-SiO_2 hybrid nanocomposites were characterized and confirmed by physico-chemical methods.

EXPERIMENTAL

Pyrene-1-carboxaldehyde (99%) and 4-nitroacetophenone (≥ 96%) were purchased from Acros Organics India Ltd. for synthesizing dinitro pyrenyl pendant pyridine. A Pd/C (10 wt.%) were procured from Alfa-Aesar India. 9-Amino carbazole, 4-hydroxy benzaldeyde and hydrazine hydrate (80%) were purchased from Loba-Chemie, India. Glacial acetic acid (99.5%), paraformaldehyde (98%), anhydrous magnesium sulphate (99%), ammonium acetate (≥ 98%), tetrahydrofuran (99.5%), and celite were procured from SRL chemicals, India. Diethyl ether (99.5%), *N*,*N*-dimethyl formamide (99%) and ethanol (99.9%) were obtained from Merck India Ltd.

Synthesis of pyrenyl pendant pyridine core aromatic diamine: The procedure reported somewhere else (**Scheme-I**) was used to synthesize pyrenyl pendant pyridine core aromatic imine [27,28]. The ^1H & ^{13}C NMR and FT-IR data characterized the structure and confirmed formation of products [29].

Synthesis of hydroxy terminal pyrenyl pendant pyridine core imine: Imine based hydroxy terminal pyrenyl pendant pyridine core derivative was synthesized by the following **Scheme-I**. In a 500 mL flask, 50 mL ethanol, pyrenyl pendant pyridine core aromatic diamine (0.001 mol, 10 g), 4-hydroxy benzaldehyde (0.002 mol, 5.40 g) were mixed to ethanol and refluxed for 4 h. The obtained mixture was quenched with water, washed using aqueous $NaHCO_3$ (200 mL). Then, the product was filtered and dried with anhydrous sodium sulphate for 10 h. Finally, hydroxyl terminal pyrenyl pendant pyridine core imine (PYPI-OH) was got after the removing residual solvent under vacuum (yield: 75%; colour: orange powder).

Synthesis of hydroxy terminal pyrenyl pendant pyridine core imine benzoxazine monomer (PYCBZ): Benzoxazine monomer from hydroxy terminal pyrenyl pendant pyridine core imine (PYCBZ) was synthesized as per **Scheme-II** [30]. In a 250 mL round bottomed flask, 50 mL dioxane, hydroxy terminal pyrenyl pendant pyridine core, PYPI-OH (0.015 mol, 10.0 g), carbazole amine (0.030 mol, 5.46 g) and formaldehyde (0.06 mol, 2.0 mL) were refluxed at 110 ºC for 6 h. The product mixture was then filtered and thoroughly washed with 1 M $NaHCO_3$ aqueous solution. The resultant product was dried under vacuum for 10 h. (Yield: 73%; colour: brown). FT-IR (KBr, ν_{max}, cm^{-1}): 3044 (=CH-), 1677 (C=C), 1322 (C-N), 1214 (C-O-C), 930 (N-CH_2-O), 747 (C-H). ^1H NMR: (400 MHz, DMSO-d_6) δ ppm: 8.67 (s, 2H), 8.58 (s, 2H), 8.20 (t, 3H), 8.15 (d, 4H), 7.76 (d, 2H), 6.91 (d, 2H) 6.72 (d, 4H), 6.10 (s, 4H), 4.64 (s, 4H). ^{13}C NMR: δ ppm: 161, 159, 149, 143, 137, 133, 129, 128, 127, 126, 121, 114, 111, 98, 68, 59 (aromatic

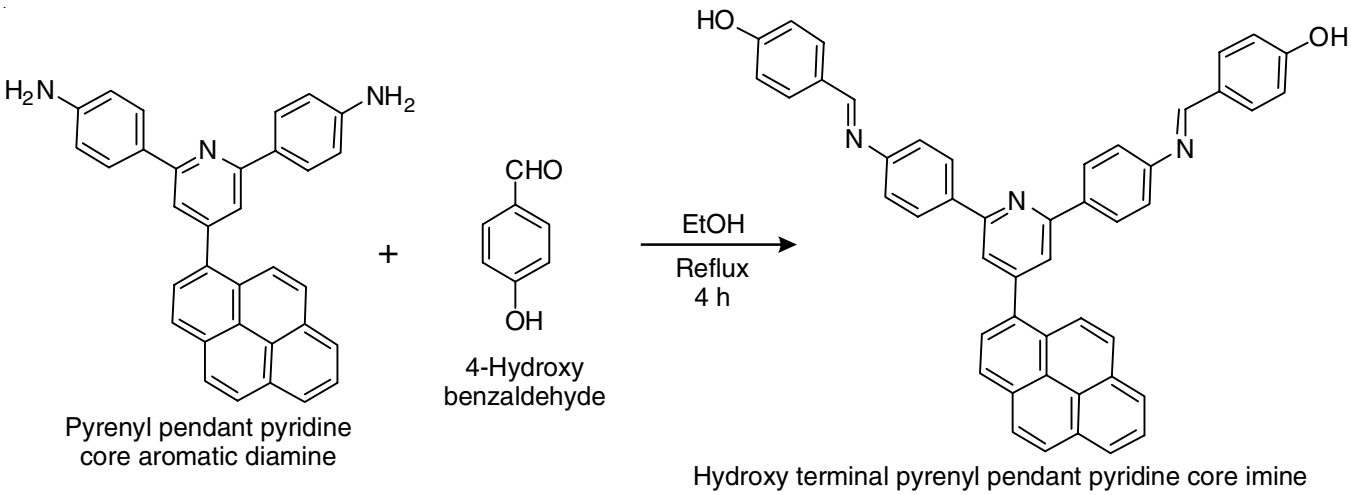

Scheme-I: Synthesis of hydroxyl terminal pyrenyl pendant pyridine core imine

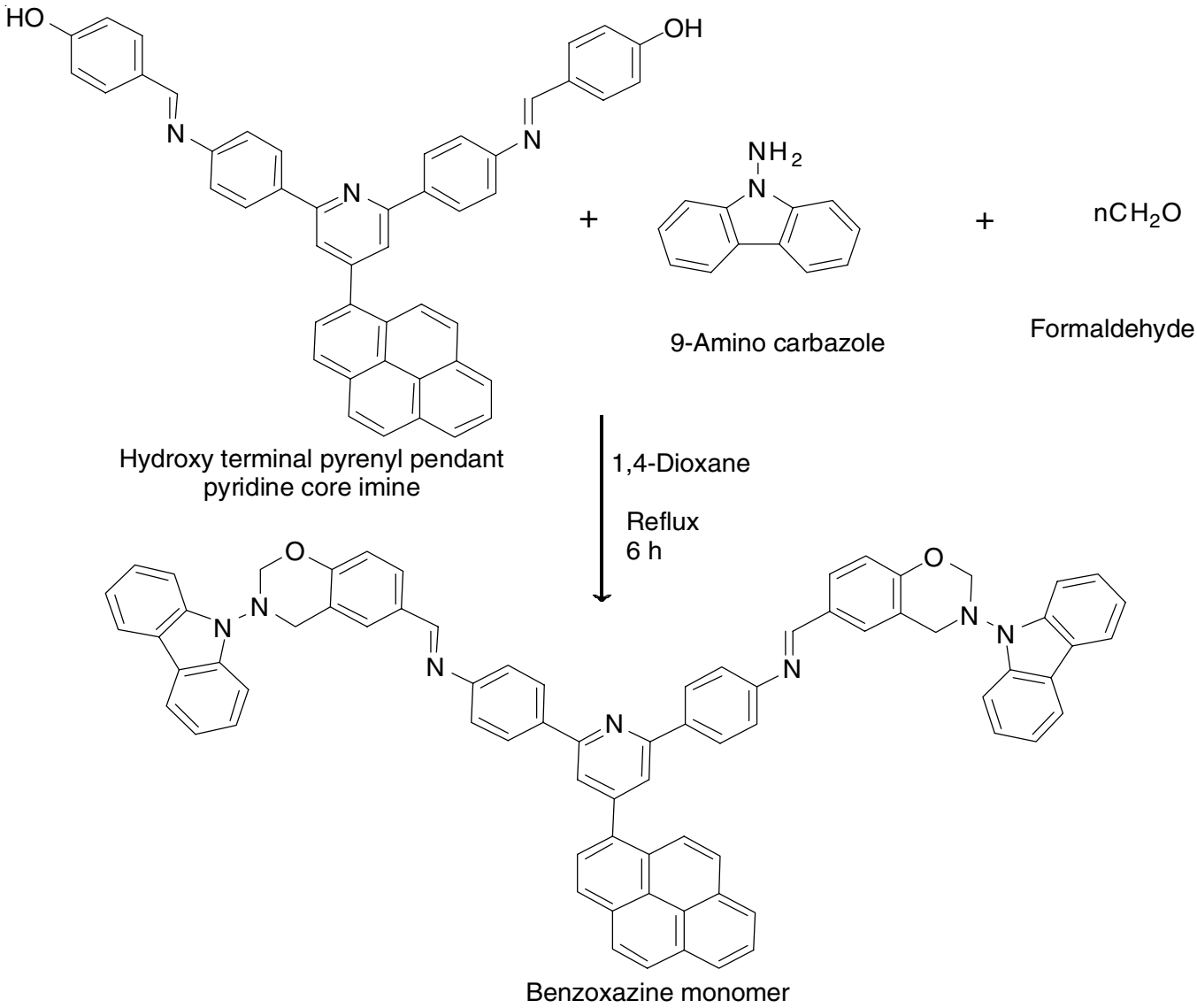

Scheme-II: Synthesis of pyrenyl pendant pyridine core imine skeletal benzoxazine monomer (BZ)

carbon). UV-visible (λ_{max}): 348 nm; Photoluminescence emission (λ_{max}): 425 nm.

Preparation of nanosilica reinforced polybenzoxazine nanocomposites: The neat polybenzoxazine (PBZ) and nanosilica reinforced polybenzoxazine (nSiO$_2$/PBZ) hybrid nanocomposites were prepared by following **Scheme-III** [27]. The benzoxazine was dissolved in 1,4-dioxane and the cured initially at 120 ºC for 120 min and then further curing was performed for 120 min at 180 ºC to get a neat PBZ matrix. The curing cycle time is shown in Table-1. The nSiO$_2$ particles were added to 1,4-dioxane along with benzoxazine monomer and the obtained homogeneous solution poured onto a precoated glass plate and then thermal ring opening polymerization was carried out at 120 ºC for 120 min and also cured at 180 ºC for 120 min to get nanosilica reinforced polybenzoxazine.

Characterization: About 100 mg of potassium bromide was finely grounded with enough quantity of the solid sample to make 1.0 wt % mixture for making KBr pellets. FT-IR spectra were recorded on a Perkin-Elmer 6X FT-IR spectrometer. The neat polybenzoxazines and nanosilica incorporated polybenzoxazine nanocomposites were characterized by UV-Vis spectrophotometer (UV-Vis) (U-4100, Hitachi, Japan). The

TABLE-1
CURING TIME CYCLE OF NANOSILICA REINFORCED POLYBENZOXAZINE NANOCOMPOSITES

Exp code	Systems	BZ (g)	nSiO$_2$ (g)	Ratio (BZ:nSiO$_2$) (w/w)	1,4-Dioxane (mL)	Curing cycle temp (°C)/min	Colour
PYCBZ	Neat PYCBZ	1.0	0	1:0	4	120 + 180 °C/120 + 120 min	Dark brown
PYCBZ$_1$	2% nSiO$_2$/PYCBZ	1.0	0.2	10:2	4	120 + 180 °C/120 + 120 min	Light brown
PYCBZ$_2$	5% nSiO$_2$/PYCBZ	0.5	0.5	1:1	4	120 + 180 °C/120 + 120 min	Light brown
PYCBZ$_3$	10% nSiO$_2$/PYCBZ	0.1	1.0	1:10	4	120 + 180 °C/120 + 120 min	Brown

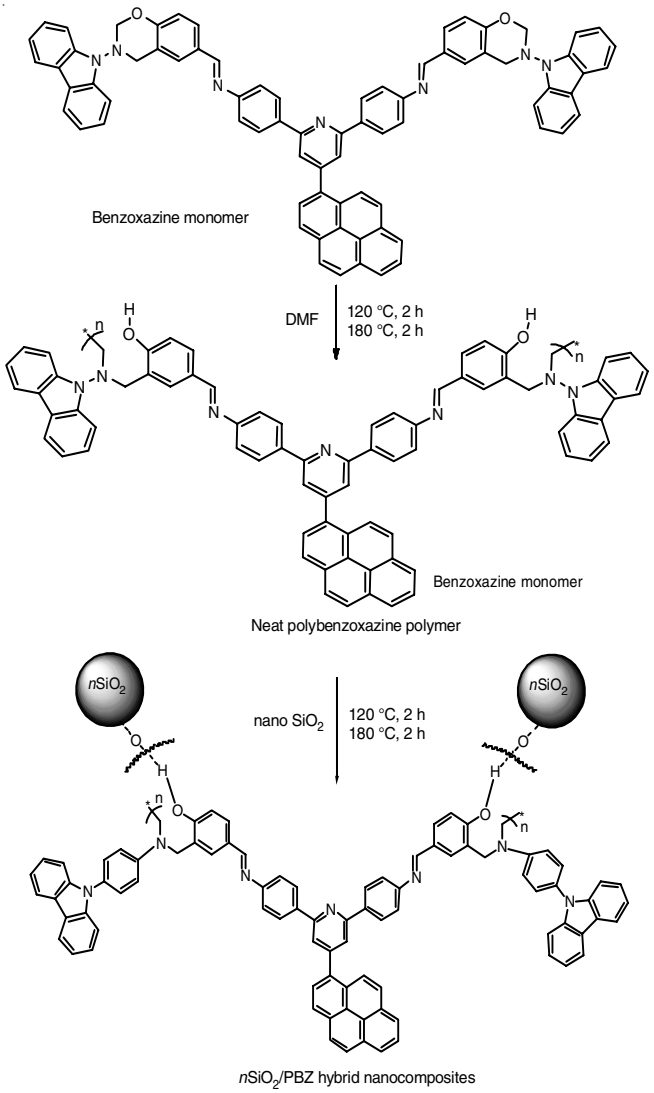

Scheme-III: Schematic representation for the Synthesis of pyrenyl pendant pyridine core imine skeletal polybenzoxazine-silica (nSiO$_2$/PBZ) hybrid nanocomposites

absorbance of the solution was measured with a wavelength ranging from 200 to 1300 nm. All ^{1}H & ^{13}C NMR analyses were done in d-CHCl$_3$ and DMSO-d_6 recorded on a Bruker 500 NMR spectrometer. The emission properties of the PBZ and PBZ-SiO$_2$ nanocomposites were also studied using fluorescence spectrophotometer (Cary Eclipse, FL1201M002, Japan) with an excitation wavelength. Scanning electron microscope (SEM) (Desktop Mini-SEM with EDS, ALFATECH), 5 kV to 30 kV variable accelerating voltage was used to observe the surface morphology of the PBZ and nSiO$_2$/PBZ nanocomposites. The transm-ission electron microscope (TEM) observations were carried on a JEOL JEM-2100 plus with an accelerating voltage of 200 kV, Emission gun-Thermionic emission (LaB_6). And Raman spectra were recorded by Micro-Raman spectrometer (785 nm laser source, HORIBA France, LABRAM HR Evolution).

Thermo gravimetric analysis (TGA) was performed in a DSC-2920 from TA Instruments coupled with a TA-2000 control system. The samples were heated at a scanning rate of 10 ºC/min under nitrogen atmosphere. A Netzsch DSC-200 differential scanning calorimeter was used for the calorimetric analysis. The instrument was calibrated with indium supplied by Netzsch. Measurements were performed under a continuous flow of nitrogen (60 mL/min). All the samples (about 10 mg in weight) were heated from ambient to 400 ºC and the thermograms were recorded at a heating rate of 10 ºC/min.

RESULTS AND DISCUSSION

Curing behaviour of benzoxazine monomer: The process of curing of benzoxazine monomer was studied by the DSC analysis is shown in Fig. 1. The DSC thermogram shows an exothermic peak, which is allotted to the benzoxazine hydroxyl group [27,29]. The onset and peak top temperature of the major peak was at 196 ºC for benzoxazine monomer, which is lower than the thermally prepared benzoxazine monomer. The peak curing temperatures of the resulting monomers were at 239 ºC (BZ) and all the benzoxazine monomers could polymerize at the temperature range of 270 ºC (BZ) as it can be seen from Fig. 1.

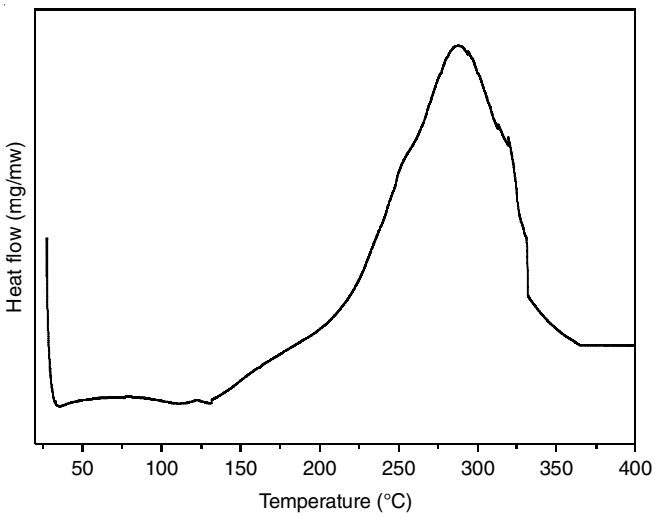

Fig. 1. Curing behaviour of benzoxazine monomer (BZ)

Characterization of nSiO$_2$/PBZ nanocomposites: The FT-IR spectrum of the neat PBZ and nSiO$_2$/PBZ nanocomposites are shown in Fig. 2. The absorption band at 3495 and 1680 cm^{-1} corresponding to the hydrogen bonded phenolic OH and a new absorption peak at 1490 cm^{-1} is due to the tetra substituted benzene ring confirmed the successful formation of polybenzoxazine matrix. The disappearance of the peaks at 940 and 1510 cm^{-1} (oxazine) and 1211 cm^{-1} (C-O-C) further confirmed the ring opening polymerization of benzoxazines [27]. The stretching vibrations of symmetric C-N and imine linkage were characterized by the peaks observed at 1333 and 1680 cm^{-1}, respectively [27-29]. The formation of nSiO$_2$/PBZ nanocomposites was evidenced from the peak formed at 1080 cm^{-1} owing to the -Si-O- linkages of nSiO$_2$ particles.

Thermal properties

Differential scanning calorimetry: Fig. 3 shows the DSC thermograms of the neat PBZ and nSiO$_2$/PBZ nanocomposites.

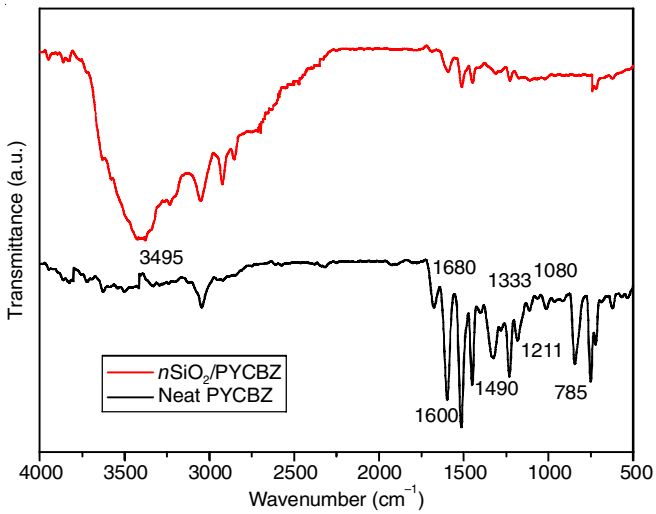

Fig. 2. FT-IR Spectra of neat PBZ and nSiO$_2$/PBZ nanocomposites

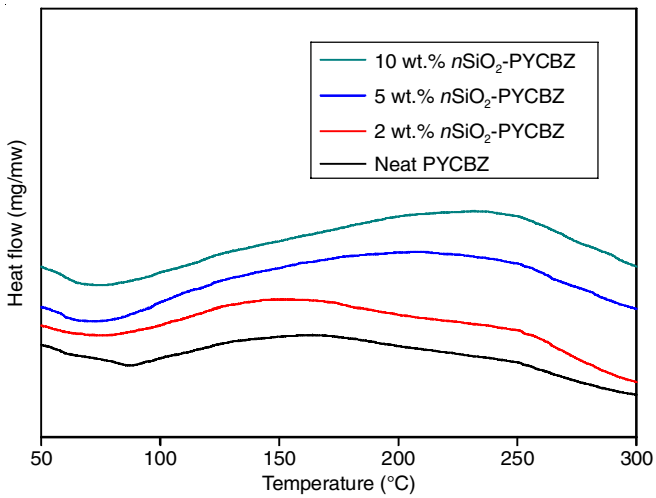

Fig. 3. DSC thermograms of neat PBZ and nSiO$_2$/PBZ nanocomposites

The glass transition temperatures (T_g) of the neat PBZ and nSiO$_2$/PBZ nanocomposites are presented in Table-2. The ring-opening polymerization of benzoxazine monomer drives faster to enhance the T_g value to the substantial level (234 ºC) accounted from the bulk organic networks. The augmentation in the glass transition temperature was exerted by the introduction of nanosilica particles into polybenzoxazine network. Thus, the T_g value of nSiO$_2$ reinforced PBZ nanocomposite was increased to about 256 ºC than that of neat PBZ system. The constrained mobility of the polymer chain network on account of the presence of hydrogen-bonding interaction will also increase the glass transition temperature of the PBZ-SiO$_2$ hybrids [16,28,31].

Thermogravimetric analysis: Thermogravimetric analysis have evidently demonstrated the enhanced thermal stability of the neat PBZ and nSiO$_2$/PBZ nanocomposites (Table-2). The initial degradation temperature of the neat PBZ hybrid was larger afforded by the existence of bulky aromatic pyrenyl and carbazole rings in the matrix (Fig. 4). The lingered decomposition rose from the homogeneously dispersed nanosilica particles onto the polybenzoxazine matrix, which led to increase the thermal stability of nSiO$_2$ reinforced PBZ nanocomposites [16,28,29,32]. The locking of the temperature withstand is escorted owing to the presence of the high bond energy and partial ionic surrounding of the Si-O-Si linkage of the dispersed nSiO$_2$ in the PBZ matrix. Furthermore, it is concluded that the higher thermal stability was supported from the formed trivial hydrogen bonding between the nanosilica particles and the benzoxazine.

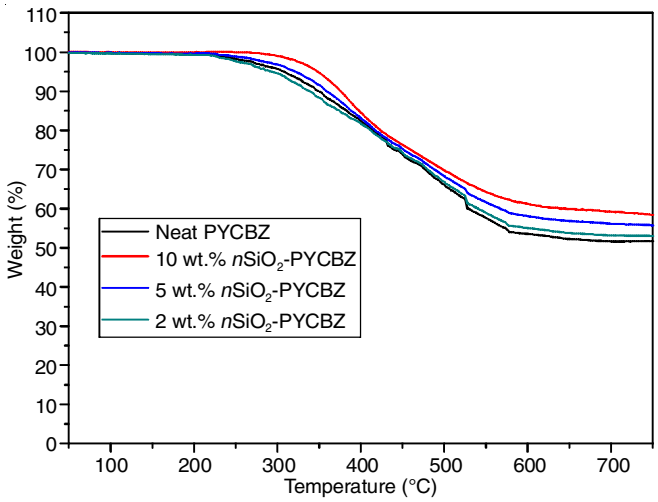

Fig. 4. TGA thermograms of neat PBZ and nSiO$_2$/PBZ nanocomposites

Limiting oxygen index: The limiting oxygen index values were calculated from TG analysis and presented in Table-2. The thermal retardancy of the neat PBZ and nSiO$_2$/PBZ nanocomposites was argued using Van Krevelen's equation (Fig. 5). An increment in the crosslinking behaviour and the presence of incorporated nanosilica particles in PBZ matrix made the higher char yielded at 700 ºC [29,33-36]. Thus, the nSiO$_2$/PBZ nanocomposites developed in the present work may be considered as good fire-retarding material for high thermal applications.

Dielectric constant: The dielectric constants of neat PBZ and nSiO$_2$/PBZ hybrid nanocomposites at 1 MHz in room temperature are shown in Table-2. The decreasing tendency of the dielectric constant in nSiO$_2$/PBZ hybrid composites

TABLE-2
THERMAL DATA OF NEAT PBZs AND nSiO$_2$/PBZ NANOCOMPOSITES

Exp. code	Systems	T_g (°C)	Char yield at 700 °C (%)	Dielectric constant (ε)	LOI at 700 °C 0.4 (σ) + 17.5	Water absorption (%)
PYCBZ	Neat PYCBZ	234	51	3.98	33.9	0.68
PYCBZ$_1$	2% nSiO$_2$/PYCBZ	236	53	3.77	34.7	0.55
PYCBZ$_2$	5% nSiO$_2$/PYCBZ	243	55	3.32	35.5	0.50
PYCBZ$_3$	10% nSiO$_2$/PYCBZ	256	58	2.53	36.9	0.44

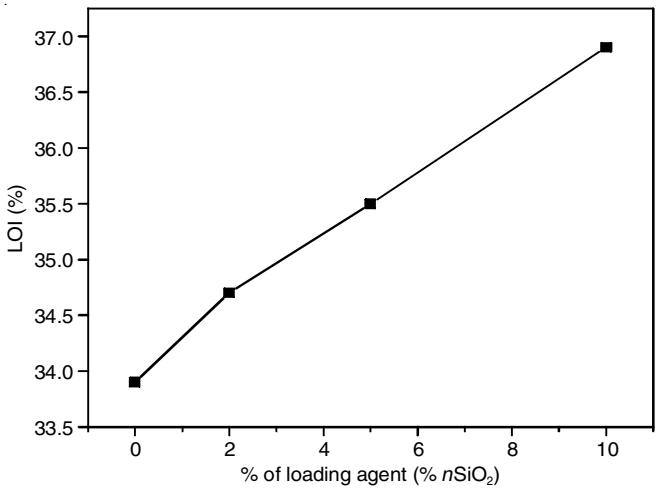

Fig. 5. LOI values of neat PBZ and nSiO$_2$/PBZ nanocomposites

designates that the addition amounts of nSiO$_2$ results in the smaller in the dipole-dipole interaction in the hybrid nanocomposites [28,34,35,37]. The decrement in the dielectric constant values (k = 2.53 for 10% of nSiO$_2$/PBZ nanocomposites is mainly attributed to the Si-O-Si linkages of nSiO$_2$ along the hybrids of the polybenzoxazine-nanosilica nanocomposites.

Water absorption behaviour: Water absorption characteristics of the neat PBZ and nSiO$_2$/PBZ composites are shown in Fig. 6. The percentage of water absorption of neat PBZ system is 0.68 %. The incorporation of inorganic nanosilica network into PBZ systems reduced the percentage of water absorption from 0.68 to 0.44 (Table-2). The decrease in percentage of water absorption may be connected with the inherent hydrophobic nature of Si-O- network present in the nSiO$_2$/PBZ composites [27,35].

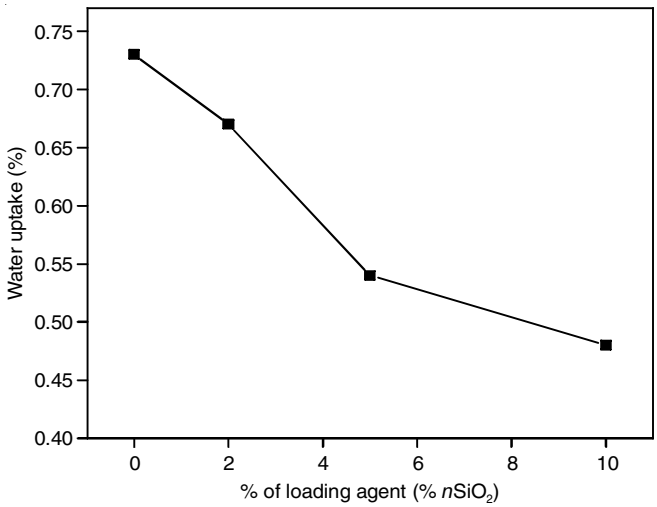

Fig. 6. Water uptake behaviour of neat PBZ and nSiO$_2$/PBZ nanocomposites

Optical properties

UV-visible absorption spectra: The UV-visible spectra of the neat PBZ and nSiO$_2$/PBZ nanocomposites are shown in Fig. 7. The absorption at 338 nm was attributed to the neat polybenzoxazine matrix with an unsymmetrical shaped peak.

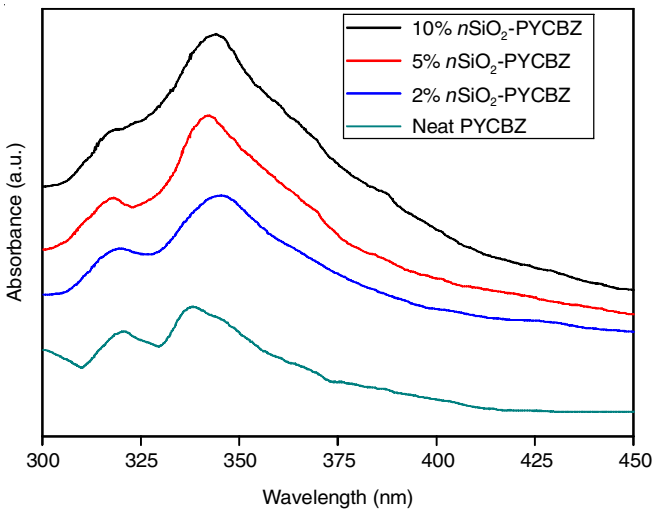

Fig. 7. UV-vis absorption spectra of neat PBZ and nSiO$_2$/PBZ nanocomposites

The incorporation of silica particles onto the PBZ matrix shifts the peak to the higher wavelength of 347 nm. The red shift confirms that the nanosilica particles were effectively reinforced throughout PBZ matrix [37].

Photoluminescence spectra: Fig. 8 represents photoluminescence spectra of the neat PBZ and nSiO$_2$/PBZ hybrid nanocomposites. The strong fluorescent emission resulted from a peak at 397 nm for PBZ and also a peak at 425 nm was found for the nSiO$_2$/PBZ nanocomposites. The shift in the emission is due to the presence of homogeneously incorporated nanosilica particles in the PBZ matrix [27,38-42]. Hence, this kind of nSiO$_2$/PBZ nanocomposite offers a wide range of applications in the fields of opto-electronics manufacturing light-emitting diode materials.

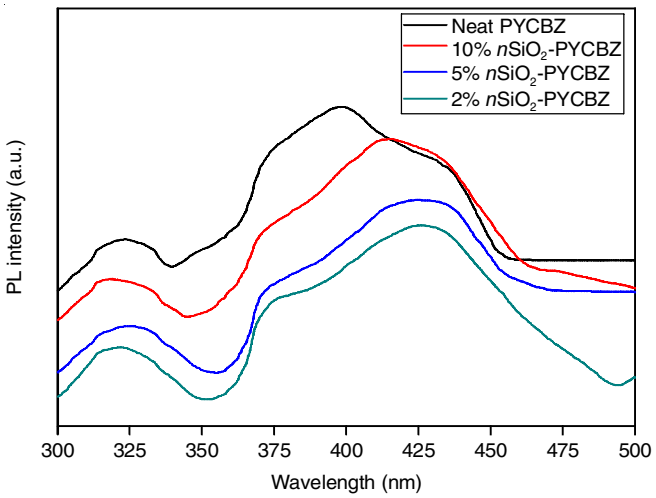

Fig. 8. Photoluminescence spectra of neat PBZ and nSiO$_2$/PBZ nanocomposites

X-Ray diffraction studies: The diffraction patterns were obtained for both the neat PBZ and nSiO$_2$/PBZ hybrid nanocomposites as shown in Fig. 9. The amorphous nature of polybenzoxazine system can be ascertained from the peak appeared at 2θ = 20.74° and also a broad amorphous peak at 20.74° for nSiO$_2$/PBZ hybrid nanocomposites, which suggested that the

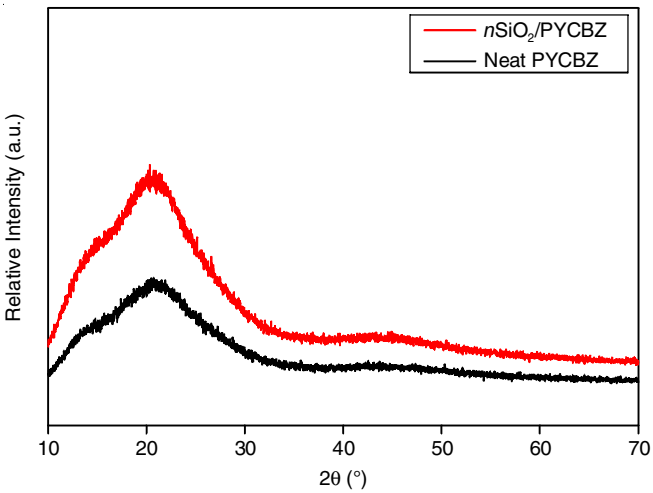

Fig. 9. XRD patterns of neat PBZ and nSiO$_2$/PBZ nanocomposites

nanosilica particles are completely dispersed in the PBZ matrix systems [27]. The minimal change in the intensity of peak owing to the uniform incorporation of nSiO$_2$ particles was evidently observed (Fig. 9). In addition, the shift in d-spacing was supported from resultant polymerization of benzoxazine and in turn with the reinforcement of nSiO$_2$ particles onto PBZ network. Furthermore, the strong covalent bonding interaction between nSiO$_2$ particles and PBZ matrix played a role in the homogenous distribution and also the retained amorphous morphology of the nanocomposites.

SEM morphology: Fig. 10 illustrates SEM analyses of the neat polybenzoxazine and nSiO$_2$ reinforced polybenzoxazine nanocomposites. It is observed that the neat PBZ systems showed an indistinguishable phase separation (Fig. 10a). The presence of distinct phase separation and localized domains inferred from the strong interfacial interaction exerted between the inorganic skeleton and the organic phase of nSiO$_2$ reinforced polybenzoxazine nanocomposites [37], which is in good agreement with XRD analysis (Fig. 9).

TEM morphology: Fig. 11 shows the TEM images of neat PBZ and nSiO$_2$ reinforced polybenzoxazine nanocomposites.

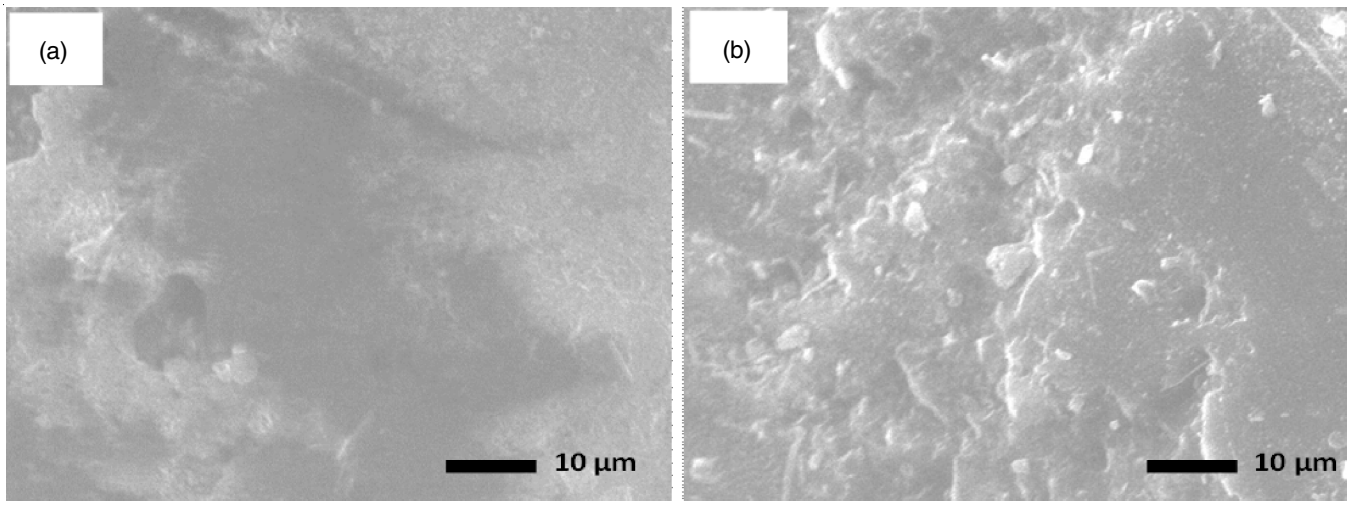

Fig. 10. SEM micrographs of (a) neat PBZ (b) nSiO$_2$/PBZ nanocomposites

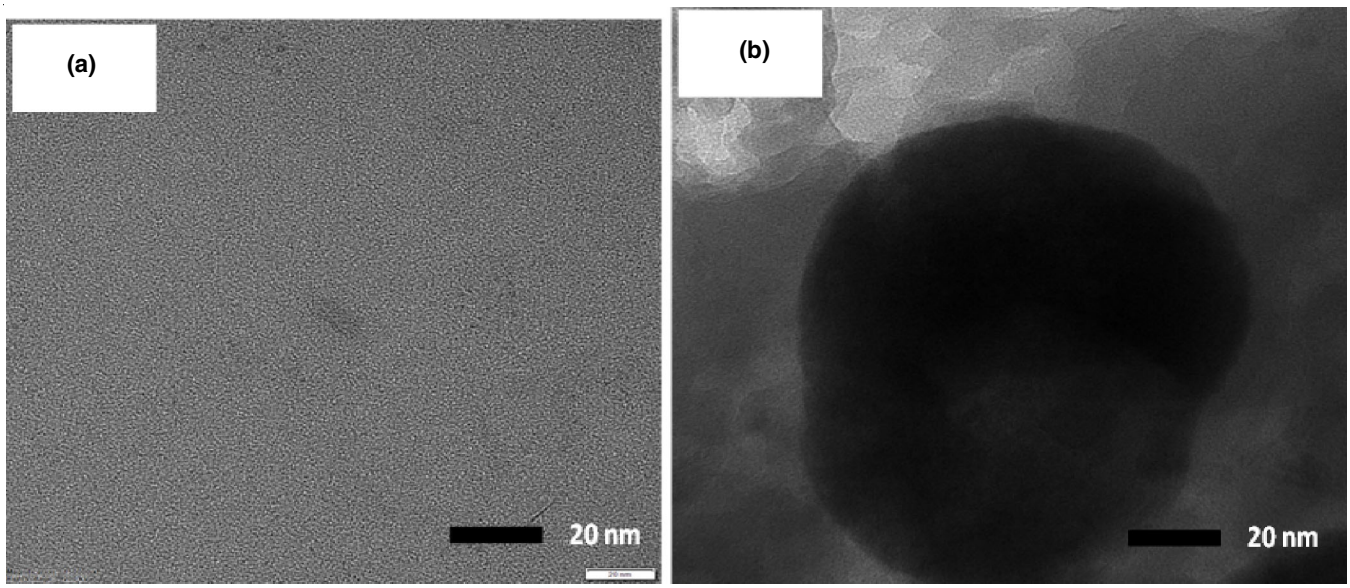

Fig. 11. TEM micrographs of (a) neat PBZ (b) nSiO$_2$/PBZ nanocomposites

These images clearly showed the successful formation of PBZ hybrid network through thermal curing. The uniform level dispersion and distribution of nanosized silica particles was achieved and confirmed surface morphology of the nanocomposites from TEM images [27,43].

Conclusion

In present work, nSiO$_2$/polybenzoxazine nanocomposites have been structurally designed and prepared from nanosilica (nSiO$_2$) and imine skeletal pyrenyl pendant pyridine core carbazole terminal benzoxazine monomer *via* thermal curing. The structural formation of hybrid nanocomposites was confirmed by various physico-chemical characterizations. The establishment of intercross linked networks resulted the elevated thermal stability and extraordinary char yield (about 50%) of hybrid nanocomposites than that of neat PBZ. The inclusion of nSiO$_2$ particles onto neat polybenzoxazine matrix enhanced the glass transition behaviour of the nSiO$_2$/PBZ hybrid nanocomposites to a temperature of 288 ºC. The decrement in the dielectric constant value was resulted from the incorporated nanosilica in the newly designed polybenzoxazine system. The effective formation of nanosized silica reinforced polybenzoxazine nanocomposites was evidenced from red shift shown by UV-Vis spectra. The photoluminescence properties of the nanocomposites were revealed from the strong fluorescent emission peak corresponding to the reinforced nSiO$_2$ particles. The existence of molecular level dispersion of nanosized silica in the PBZ hybrid system was confirmed by XRD studies. The molecular level reinforcement of nSiO$_2$ particles in the PBZ network was ascertained from SEM images. The TEM images displayed the parent surface morphology of nSiO$_2$ after incorporating with PBZ matrix. Thus, this nSiO$_2$/polybenzoxazine nanocomposite may be look forward to find a wide range of applications in the fields of high-temperature EMI shielding, microelectronics and aerospace.

ACKNOWLEDGEMENTS

The authors acknowledge SRM Institute of Science and Technology for providing XRD, photoluminescence, HRTEM and micro-Raman facilities and MNRE Project No. 31/03/2014-15/PVSE-R&D Government of India for TEM analysis.

CONFLICT OF INTEREST

The authors declare that there is no conflict of interests regarding the publication of this article.

REFERENCES

1. H. Zou, S. Wu and J. Shen, *Chem. Rev.*, **108**, 3893 (2008); https://doi.org/10.1021/cr068035q
2. Y. Lin, J. Jin, M. Song, S.J. Shaw and C.A. Stone, *Polymer (Guildf.)*, **52**, 1716 (2011); https://doi.org/10.1016/j.polymer.2011.02.041
3. S. Zhang, Y. Yan, X. Li, H. Fan, Q. Ran, Q. Fu and Y. Gu, *Eur. Polym. J.*, **103**, 124 (2018); https://doi.org/10.1016/j.eurpolymj.2018.03.013
4. S.B. Shen and H. Ishida, *J. Polym. Sci., B, Polym. Phys.*, **37**, 3257 (1999); https://doi.org/10.1002/(SICI)1099-0488(19991201)37:23<3257::AID-POLB1>3.0.CO;2-0
5. K.S. Santhosh Kumar, C.P. Reghunadhan Nair, R. Sadhana and K.N. Ninan, *Eur. Polym. J.*, **43**, 5084 (2007); https://doi.org/10.1016/j.eurpolymj.2007.09.012
6. T. Lakshmikandhan, A. Chandramohan, K. Sethuraman and M. Alagar, *Des. Monomers Polym.*, **19**, 67 (2016); https://doi.org/10.1080/15685551.2015.1092014
7. C.F. Wang, Y.T. Wang, P.H. Tung, S.W. Kuo, C.H. Lin, Y.C. Sheen and F.C. Chang, *Langmuir*, **22**, 8289 (2006); https://doi.org/10.1021/la061480w
8. H. Oie, A. Sudo and T. Endo, *J. Polym. Sci. A Polym. Chem.*, **48**, 5357 (2010); https://doi.org/10.1002/pola.24338
9. Y. Jiang, S. Yan, Y. Chen and S. Li, *J. Adhes. Sci. Technol.*, **33**, 1974 (2019); https://doi.org/10.1080/01694243.2019.1623434
10. H. Ishida and H.Y. Low, *J. Appl. Polym. Sci.*, **69**, 2559 (1998); https://doi.org/10.1002/(SICI)1097-4628(19980926)69:13<2559::AID-APP5>3.0.CO;2-9
11. T. Agag and T. Takeichi, *Polymer*, **52**, 2757 (2011); https://doi.org/10.1016/j.polymer.2011.04.044
12. C. Schramm, B. Rinderer, R. Tessadri and H. Duelli, *J. Sol-Gel Sci. Technol.*, **53**, 579 (2010); https://doi.org/10.1007/s10971-009-2135-7
13. M. Selvi, S. Devaraju, M.R. Vengatesan and M. Alagar, *J. Sol-Gel Sci. Technol.*, **72**, 518 (2014); https://doi.org/10.1007/s10971-014-3467-5
14. T. Agag and T. Takeichi, *Polym. Compos.*, **29**, 750 (2008); https://doi.org/10.1002/pc.20448
15. M.R. Vengatesan, S. Devaraju, K. Dinakaran and M. Alagar, *Polym. Compos.*, **32**, 1701 (2011); https://doi.org/10.1002/pc.21177
16. M. Selvi, M.R. Vengatesan, S. Devaraju, M. Kumar and M. Alagar, *RSC Adv.*, **4**, 8446 (2014); https://doi.org/10.1039/c3ra44511a
17. S. Jothibasu, A.A. Kumar and M. Alagar, *High Perform. Polym.*, **23**, 11 (2011); https://doi.org/10.1177/0954008310389838
18. R.P. Priya, S.G. Gunasekaran and M. Dharmendirakumar, *J. Nanosci. Nanotechnol.*, **15**, 9509 (2015); https://doi.org/10.1166/jnn.2015.10741
19. S. Devaraju, M.R. Vengatesan, A.A. Kumar and M. Alagar, *J. Sol-Gel Sci. Technol.*, **60**, 33 (2011); https://doi.org/10.1007/s10971-011-2547-z
20. V. Selvaraj, K.P. Jayanthi, T. Lakshmikandhan and M. Alagar, *RSC Adv.*, **5**, 48898 (2015); https://doi.org/10.1039/C5RA07480K
21. K.S. Santhosh Kumar, C.P. Reghunadhan Nair and K.N. Ninan, *Eur. Polym. J.*, **45**, 494 (2009); https://doi.org/10.1016/j.eurpolymj.2008.11.001
22. Y. Wang, K. Kou, Z. Li, G. Wu, Y. Zhang and A. Feng, *High Perform. Polym.*, **28**, 1235, (2016); https://doi.org/10.1177/0954008315623353
23. H. Ardhyananta, M.H. Wahid, M. Sasaki, T. Agag, T. Kawauchi, H. Ismail and T. Takeichi, *Polymer*, **49**, 4585 (2008); https://doi.org/10.1016/j.polymer.2008.08.030
24. K. Adachi, A. Achimuthu and Y. Chujo, *Macromolecules*, **37**, 9793 (2004); https://doi.org/10.1021/ma0400618
25. T. Agag, H. Tsuchiya and T. Takeichi, *Polymer*, **45**, 7903 (2004); https://doi.org/10.1016/j.polymer.2004.09.022
26. S.G. Gunasekaran, V. Arivalagan, M. Dharmendirakumar and L.D. Stephen, *J. Nanosci. Nanotechnol.*, **17**, 5271 (2017); https://doi.org/10.1166/jnn.2017.13810
27. S.G. Gunasekaran, K. Rajakumar and M. Dharmendirakumar, *Polym. Plast. Technol. Eng.*, **54**, 989 (2015); https://doi.org/10.1080/03602559.2014.974281
28. S.G. Gunasekaran, K. Rajakumar, M. Dharmendirakumar and M. Alagar, *Int. J. Plast. Technol.*, **19**, 309 (2015); https://doi.org/10.1007/s12588-015-9111-6
29. N. Amutha and M. Sarojadevi, *J. Polym. Res.*, **15**, 487 (2008); https://doi.org/10.1007/s10965-008-9193-3

30. S.G. Gunasekaran, K. Rajakumar and M. Dharmendirakumar, *Int. J. Nanosci.*, **14**, 1550021 (2015); https://doi.org/10.1142/S0219581X15500210
31. R. Hariharan, S. Bhuvana, M.A. Malbi and M. Sarojadevi, *J. Appl. Polym. Sci.*, **93**, 1846 (2004); https://doi.org/10.1002/app.20650
32. S. Yan, W. Chen, X. Yang, C. Chen, M. Huang, Z. Xu, K.W.K. Yeung and C.F. Yi, *Polym. Bull.*, **66**, 1191 (2011); https://doi.org/10.1007/s00289-010-0343-5
33. T. Agag and T. Takeichi, *J. Polym. Sci. A Polym. Chem.*, **44**, 1424 (2006); https://doi.org/10.1002/pola.21245
34. T. Hanemann and D.V. Szabo, *Materials*, **3**, 3468 (2010); https://doi.org/10.3390/ma3063468
35. S.G. Gunasekaran, K. Rajakumar, M. Dharmendirakumar and M. Alagar, *J. Polym. Res.*, **21**, 342 (2014); https://doi.org/10.1007/s10965-013-0342-y
36. D. Zhuo, A. Gu, G. Liang, J. Hu, L. Cao and L. Yuan, *Polym. Degrad. Stab.*, **96**, 505 (2011); https://doi.org/10.1016/j.polymdegradstab.2011.01.006
37. R. Sasikumar, N. Padmanathan and M. Alagar, *New J. Chem.*, **39**, 3995 (2015); https://doi.org/10.1039/C4NJ02188F
38. H. Ardhyananta, T. Kawauchi, T. Takeichi and H. Ismail, *High Perform. Polym.*, **22**, 609 (2010); https://doi.org/10.1177/0954008309354129
39. T. Agag and T. Takeichi, *Polymer (Guildf.)*, **41**, 7083 (2000); https://doi.org/10.1016/S0032-3861(00)00064-1
40. S. Devaraju, M.R. Vengatesan, M. Selvi, A.A. Kumar, I. Hamerton, J.S. Go and M. Alagar, *RSC Adv.*, **3**, 12915 (2013); https://doi.org/10.1039/c3ra41144c
41. J. Narayanan, M.J. Jungman and D.L. Patton, *React. Funct. Polym.*, **72**, 799 (2012); https://doi.org/10.1016/j.reactfunctpolym.2012.07.012
42. S. Devaraju, M.R. Vengatesan, M. Selvi, J.K. Song and M. Alagar, *Polym. Compos.*, **34**, 904 (2013); https://doi.org/10.1002/pc.22496
43. T.P. Jung, A.S. Jin, H.A. Sung, H.K. Jong and W.K. Sang, *J. Ind. Eng. Chem.*, **16**, 517 (2010); https://doi.org/10.1016/j.jiec.2010.03.030